ORGANIC CHEMISTRY FRONTIERS

RESEARCH ARTICLE

View Article Online
View Journal | View Issue

Cite this: *Org. Chem. Front.*, 2025, **12**, 6852

New mode of sulfur ylides reactivity: stereoelectronic control provides C–C bond insertion before cyclopropanation/epoxidation directly affording homologated three-membered rings

Vitaly V. Shorokhov, [a] Beauty K. Chabuka, [b] Albina A. Nikolaeva,[a] Sergey S. Zhokhov, [a] Ivan A. Andreev, [c] Nina K. Ratmanova, [c] Igor V. Trushkov, *[c] Olga A. Ivanova *[a] and Igor V. Alabugin *[b]

Received 5th September 2025,
Accepted 26th September 2025

DOI: 10.1039/d5qo01266j

rsc.li/frontiers-organic

Ylides are versatile reagents known for their dual electrophilic and nucleophilic reactivity, mimicking carbenes in many reactions. In this study, we uncover a previously unreported reactivity pathway for ylides: a methylene insertion into C–C bonds. We show that sulfur ylides can achieve homologation of alkenes and aldehydes before proceeding through the classical Corey–Chaykovsky reaction. This process allows for the dual transfer of CH_2 groups to both substrates, yielding benzylcyclopropanes and benzyloxiranes, valuable intermediates in organic synthesis. Remarkably, the same sulfur ylide reagent participates in two distinct carbene-like transformations within this cascade. Mechanistic studies reveal the role of a tightly coordinated stereoelectronic network playing a crucial role in facilitating anionic 1,2-aryl shifts.

Introduction

Ylides, $L_nX^+–C^–R^1R^2$, are chameleonic chemical species that combine nucleophilic and electrophilic properties, arising from their unique electronic structures. The ability of ylides to stabilize charge separation while remaining reactive makes them indispensable for constructing complex organic molecules through a wide range of transformations.[1]

Ylides share several intriguing connections with carbenes and can, in fact, be described as products of a reaction between a Lewis base and a carbene. This connection is further reflected in their reactivity patterns: like singlet carbenes, ylides exhibit both electrophilic and nucleophilic properties at the same carbon atom. Carbenes possess a lone pair and an empty p-orbital, whereas ylides display a lone pair geminal to an electron-deficient leaving group, L_nX (Scheme 1A).

As a result, ylides act as synthetic equivalents of carbenes in a number of processes, both with and without transition metals.[2–5] Their carbene-like reactivity is exemplified by the formation of three-membered rings in the classic Corey–Chaykovsky reaction (CCR) of sulfur ylides with aldehydes, ketones, imines, and electron-depleted alkenes.[6–9] Other examples of carbene-like reactivity, such as ylide insertions into C–H, N–H, S–H, and similar bonds, are less common but also documented.[2–4] However, to the best of our knowledge, the insertion of ylides into C–C bonds has not been reported to date,[10] despite this process being well-known for carbenes.[11–14]

The reactivity of ylides depends on the nature of the heteroatom X and the substituents on the carbon atom (Scheme 1B).[15] For example, pyridinium ylides form simple 1,2-adducts in reactions with aldehydes[16,17] and indolizines with acceptor alkenes.[18–20] Phosphonium ylides[21,22] generally do not react with electron-deficient alkenes but readily convert carbonyl compounds into alkenes (the Wittig reaction). In contrast, sulfur ylides[23–25] react efficiently with both aldehydes and electrophilic alkenes to form three-membered rings. These differences arise from divergent pathways stemming from a common betaine intermediate, which can either be trapped *via* proton transfer to form *N*-ylides or undergo a cyclization (3-*exo* for *S*-ylides and 4-*endo* for *P*-ylides). In the search for new interrupted and extended versions of CCR[26–30] and CCR-based routes to donor–acceptor cyclopropanes,[31–40] we have discovered a few reactivity modes associated with additional functionalities.[41–43]

In this study, we introduce a previously unobserved reactivity pathway for the parent betaine species: a 1,2-shift leading to the formal insertion of a CH_2 group into a C–C bond

[a]*Department of Chemistry, M. V. Lomonosov Moscow State University, Leninskie gory 1-3, Moscow 119991, Russia. E-mail: iv@kinet.chem.msu.ru*
[b]*Department of Chemistry and Biochemistry, Florida State University, Tallahassee, Florida 32306-4390, USA. E-mail: alabugin@chem.fsu.edu*
[c]*N. D. Zelinsky Institute of Organic Chemistry Russian Academy of Sciences, Leninsky pr. 47, Moscow 119991, Russia*

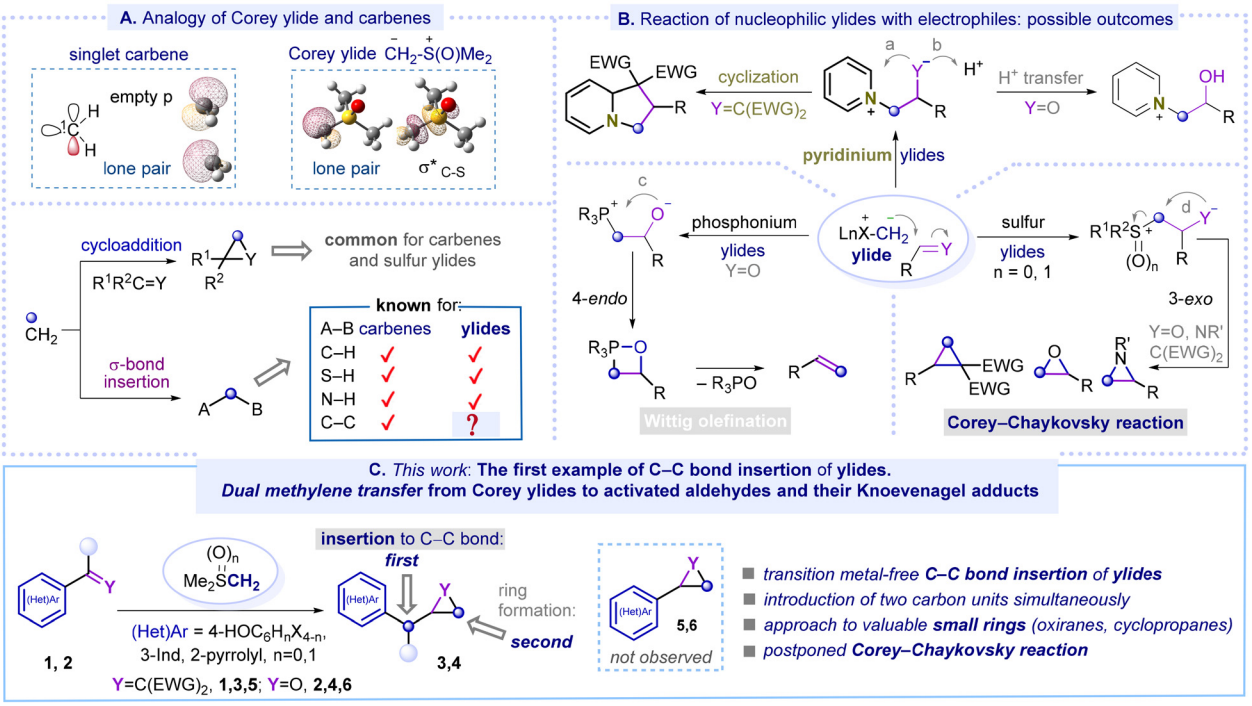

Scheme 1 A. Ylides can be considered as carbene equivalents. B. Diverging synthetic routes from a common betaine intermediate in ylide reactions with π-electrophiles. C. This work reports CH_2 group insertion into a C(Ar)–C(=Y) bond, followed by the Corey–Chaykovsky reaction to form benzylcyclopropanes. Alternatively, a similar procedure applied to aryl aldehydes affords benzyloxiranes.

(Scheme 1C). As this new path preserves the alkene moiety, the homologated product is primed for the classic Corey–Chaykovsky cyclopropanation in the subsequent step. This unprecedented cascade thus enables a dual CH_2 transfer from sulfur ylides to push–pull alkenes **1** *via* both bond insertion and cyclopropanation. A similar procedure can also be applied to (het)aryl aldehydes and ketones **2**, further increasing the utility of this sequence and providing an approach to valuable small rings **3**, **4**.

In this work, we explore the scope and limitations of these reactions in combination with mechanistic and computational analysis. Our findings reveal why the *para*-hydroxyaryl group or similar NH-acidic activating moiety is essential for transferring two CH_2 groups to both alkenes and carbonyl compounds. Furthermore, we uncover a general stereoelectronic pattern, where synergistic contributions of multiple functionalities collectively enable the unprecedented homologation step before the reaction proceeds along the CCR pathway.

Results and discussion

This study started with a serendipitous discovery that *p*-hydroxybenzylidenemalonate **1a** reacts with dimethylsulfoxonium methylide (DMSOM) to form homologated analogue **3a** rather than the expected 4-hydroxyaryl cyclopropane **5**. Intrigued by this finding, we decided to explore the scope and limitations of this process.

Dual methylene transfer to alkenes: homologation and cyclopropanation

To optimize the conditions for the dual methylene group transfer, we selected the transformation of alkene **1a** to cyclopropane **3a** as the model reaction. We systematically varied parameters, such as solvent, base, reaction time, temperature, substrate concentration, reagent loading, and the order of reagent and substrate addition (see Table S1). The optimal procedure was found to involve the addition of freshly prepared ylide to the deprotonated phenol-substituted alkene at 55 °C, as described in the SI. Under optimized conditions, we studied the scope of this process using diverse substituted 4-hydroxybenzylidenemalonates (Scheme 2A). Alkyl and alkoxy groups at the C(3) and C(5) atoms of the aromatic ring were well-tolerated under the reaction conditions; compounds **3b**,**d**,**e** were obtained in 75–87% yields. The 3,4-dihydroxyphenyl-substituted alkene, however, furnished the product **3c** in slightly lower yield (64%). Halogen atom at the C(3) position also reduced the yield of **3** (53–58% for **3f–h**). The presence of two halogen atoms at both *meta*-positions caused a substantial yield drop, with **3i** obtained in only 11%. In contrast, varying the ester groups in compound **1** had minimal impact on the reaction yield, resulting in 76–78% yields for **3j** and **3k**. However, substituting one ester group with a cyano or dialkoxyphosphoryl group decreased the yields of the target products to 53% for **3l** and 35% for **3m**. Comments on these and some other results are given below, since an understanding of the reaction mechanism is highly desirable for a good explanation

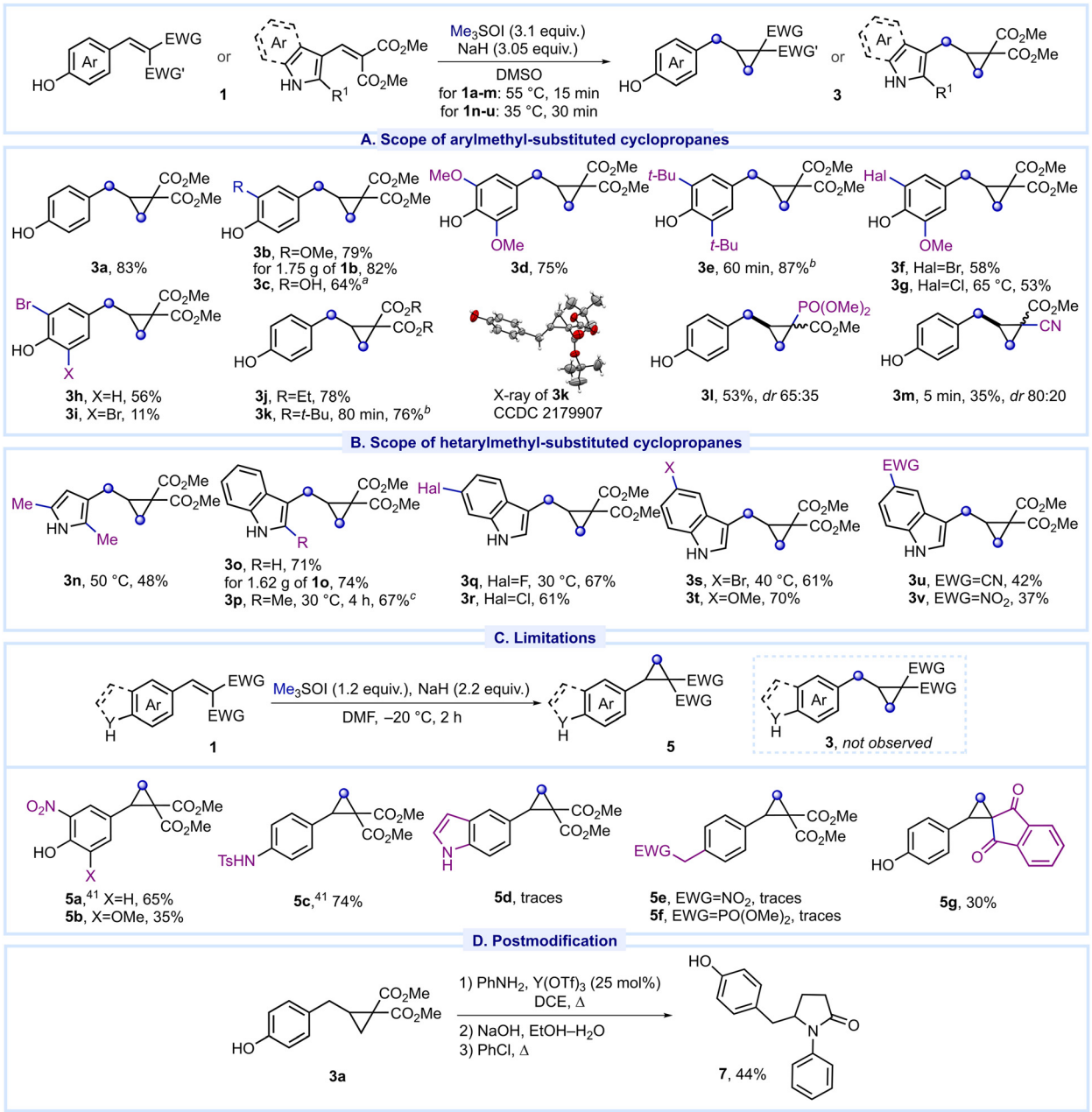

Scheme 2 Scope and limitations of dual methylene group transfer, providing benzyl- and hetarylmethyl-substituted cyclopropanes. Reaction conditions: NaH was added to the solution of Me_3SOI, the mixture was stirred for 40 min; the obtained ylide was added to 0.15 M solution of **1** in the same solvent; reagents loading, reaction temperature and time are given in reaction schemes, if other not specified. [a] 3.1 equiv. of Me_3SOI and 4.05 equiv. of NaH were used. [b] 3.5 equiv. of Me_3SOI and NaH were used. [c] 4.0 equiv. of Me_3SOI and 4.3 equiv. of NaH were used; yield after treatment of partially hydrolyzed product with CH_3I (1.0 equiv.), K_2CO_3 (0.5 equiv.), DMF, rt, 3 h is given.

of the influence of the nature of the substrates on the reaction outcome.

We hypothesized that the unusual dual methylene group transfer to substrates **1** arises from modifications of the Corey–Chaykovsky intermediate due to the deprotonation of the 4-hydroxy group. Following this rationale, we supposed that *N*-unsubstituted 3-indolyl- and 3-pyrrolyl-substituted acceptor alkenes could also be effective in the reaction as nitrogen deprotonation in these substrates should lead to the related quinonoid intermediate. Indeed, pyrrole **1n** and a series of indoles **1o–v** successfully produced the desired products **3** (Scheme 2B). Substrates with electron-withdrawing groups at the C(5) position of the indole ring gave low yields, while those with a 5-methoxy group or without a substituent delivered products in approximately 70% yields. Indoles with halogens at the C(5) or C(6) atoms, as well as 2-substituted indoles (**1p–s**), showed similar efficiency. Finally, using compounds **1b** and **1o** we demonstrated that the synthesis of benzylcyclopropanes

and (1*H*-indol-3-yl)methyl-substituted cyclopropanes **3** can be scaled without significant changes in the yield of the target products (82% and 74% from 1.75 g and 1.62 g of the starting materials, respectively).

At the same time, several limitations of this reaction were identified (Scheme 2C). Specifically, 3-nitro-4-hydroxyphenyl-substituted alkenes **1w**,**x** afforded only polymeric products under the standard conditions and 2-arylcyclopropanes **5a**,**b** when the reaction was carried out at −20 °C. Similarly, 2-arylcyclopropane **5c** was obtained from the *p*-(tosylamino)phenyl-substituted substrate, even though the tosylamino group often behaves similarly to a phenoxy group.[41,44] We also investigated alkenes containing 5-indolyl and 4-XCH_2-phenyl groups wherein X = NO_2, $PO(OMe)_2$, but neither products **3** nor compounds **5** were obtained from these substrates. Lastly, 2-(4-hydroxybenzylidene)indane-1,3-dione produced 2-arylcyclopropane **5g**, albeit with a modest 30% yield (Scheme 2).

The target cyclopropanes **3** represent a new subclass of DA cyclopropanes with underexplored reactivity. We found that **3a** readily undergoes ring opening/recyclization with aniline.[45,46] Thus, a telescoped three-step sequence yields tyramine **7** with an embedded pyrrolidone residue in 44% total yield.

Mechanistic and computational studies

To clarify the reaction mechanism, we carried out control experiments (Scheme 3A). The reaction of **1a** with perdeuterated DMSOM gave rise to **3a-*d*$_4$** with deuterium atoms at both methylene groups. Treating substrate **1a** with 1 equivalent of DMSOM afforded benzylcyclopropane **3a** in 43% yield, with 48% of unreacted **1a** recovered. This means that the conversion of intermediates formed in this reaction to products proceeds faster than the formation of intermediates from **1a**. The reaction of DMSOM with (3-hydroxybenzylidene)malonate **1ad** produced non-homologated arylcyclopropane **3h**, underscoring the critical role of the *para*-hydroxy group. In contrast, the reaction of DMSOM with 2-acetoxyphenyl-substituted alkene **1ae**, which is also likely to involve a phenolate intermediate, produced a complex mixture of unidentified products. The for-

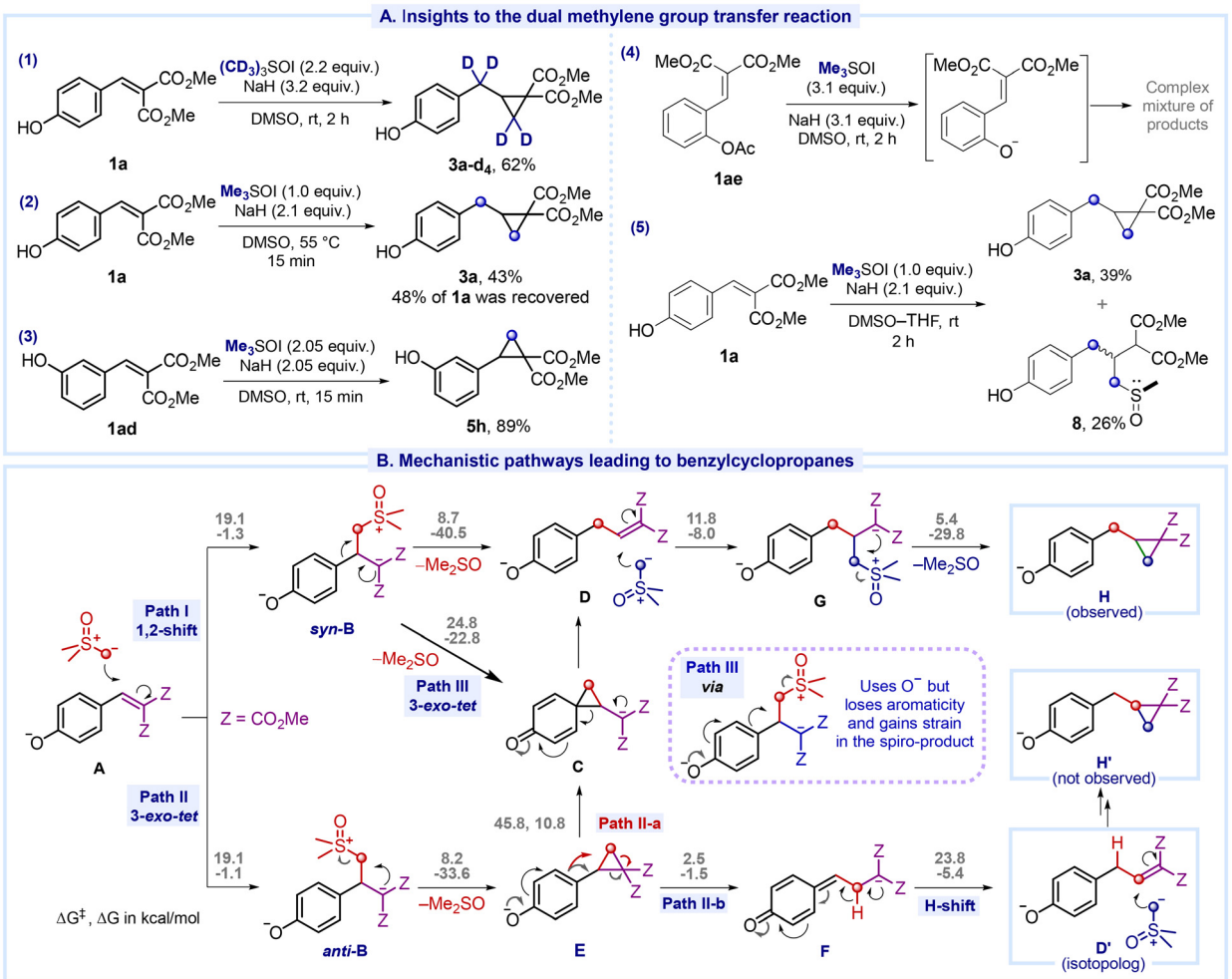

Scheme 3 A. Experimental probes in the mechanism of dual methylene group transfer. B. Three scenarios and calculated Δ*G* values for the phenoxide/ylide reaction (**Paths I–III**). **Paths I** and **III** would lead to the experimentally observed product, whereas **Path II** would lead to its isotopolog (Z = CO_2Me).

mation of S–O-adduct **8** under non-optimized conditions provides evidence for the generation of an intermediate **G**. **Paths I** and **III** lead to the experimentally observed product and the classic Corey–Chaykovsky **Path II** leads to its isotopolog (Scheme 3B). The first step involves a nucleophilic ylide attacking the electrophilic C=C bond and forming an intermediate **B** with multiple reactivity options. The *syn*- and *anti*-conformers of **B** are close in energy but stereoelectronically primed for different reactions. ***Syn*-B** can form the intermediate **D** either directly *via* a 1,2-aryl shift (**Path I**) or indirectly through a 3-*exo-tet* cyclization with participation of the aryl group that forms spirocyclopropane **C** (**Path III**). Formation of **D** completes the formal CH_2 insertion between the aryl group and the alkene moiety of the reactant. On the other hand, ***anti*-B** undergoes a 3-*exo-tet* cyclization with the enolate to form an isomeric cyclopropane **E** (**Path II**), *i.e.*, the usual Corey–Chaykovsky product.

To gain deeper insights, we studied the energy profile for the transformation of **1a** into **3a** at the B3LYP/D4/6-311++G(d, p)/CPCM(DMSO) level of theory (Scheme 3B).[47–52]

Indeed, computational analysis identified three possible paths to the final products. Due to the loss of aromaticity in the benzene ring, **Path III** has a much higher activation barrier (24.8 kcal mol^{-1}) than **Paths I** (8.7 kcal mol^{-1}) and **II** (8.2 kcal mol^{-1}). However, the small difference between the latter ($\Delta\Delta G^{\ddagger}$ = 0.5 kcal mol^{-1}) is inconsistent with the experimental preferences, motivating us to explore the competition between **Paths I** and **II** deeper. Analyzing the nature of the two transition states turns out to be instrumental in understanding this interesting reactivity puzzle. Importantly, crossing from **Path II** to **Path I** is energetically unlikely, as both **D** and **E** are ~20 kcal mol^{-1} lower than the dearomatized intermediate **C** connecting them. Hence, the competition between **Paths I** and **II** must be kinetic and is not explained by the reaction models presented in Scheme 3.

How to make 1,2-shift fast? Stereoelectronic lessons

The 3-*exo-tet* cyclizations (**Paths II** and **III**) are straightforward S_N2-like reactions, involving the same leaving group and one of the two anionic nucleophilic centers. In **Path II**, the enolate acts as the nucleophile, while in **Path III**, the phenolate takes this role. Due to the unfavorable loss of aromaticity, the phenolate loses to the enolate, making **Path II** preferred. However, the 1,2-shift transition state (**Path I**) is intriguing. Here, several stereoelectronic factors work together to make this previously unobserved pathway possible. As the 1,2 Ar-shift must break a relatively strong $C(sp^2)$–$C(sp^3)$ bond, it requires assistance from more than one source. Because both the enolate donor and the σ^*_{C-S} orbitals interact *via* the breaking C–C bond, this process requires the coplanarity of these three orbitals. To show the generality of such stereoelectronic factors, we compare the orbital network responsible for the 1,2-shift in the new reaction and the classic Bayer–Villiger rearrangement (BVR) (Fig. 1A), where a similar 1,2-shift occurs. BVR is facilitated by two stereoelectronic effects[53–56] which include the p-type lone pair of O^1, the breaking C–R_m bond and the O^3–O^4 acceptor. The "primary stereoelectronic effect" is activated when the breaking O–O bond is aligned antiperiplanar to the migrating C–R_m bond while the "secondary effect" requires the lone pair on the O^1 group to be in proper alignment with the breaking C–R_m bond. These two effects work together to ensure smooth electron flow from the donor to the acceptor. Specifically, donation from the lone pair on O^1 aids in breaking the C–R_m bond as the R_m group shifts to O^3 and the O^3–O^4 bond cleaves. Consequently, the O^1=C and R_m–O^3 bonds are formed in a concerted manner. Furthermore, the same donor assistance is achieved with deprotonated nitrogen in 3-indolyl and 3-pyrrolyl substituents (Scheme 4).

The unmistakable similarity between the two 1,2-shifts points out the generality of such stereoelectronic networks. Both 1,2-shifts transfer electron density from a non-bonding orbital (O lone pair in BVR *vs*. carbanion in the reaction under discussion) to a departing leaving group (OR for BVR *vs*. DMSO here). In the absence of a direct connection between the donor and acceptor, the migrating bond serves as a relay to transfer the electron density between two functional groups. The fact that the lessons from the stereoelectronic analysis of the Criegee intermediate transcend the BVR highlights once again the broad utility of stereoelectronic effects in organic reaction design.[57–59]

Role of oxygen anion in 1,2-shift transition state

However, the stereoelectronic network described above is necessary but not sufficient to enable the 1,2-shift. The presence of the *para*-OH group on the benzene ring plays a crucial additional role (Fig. 1B). This role is illustrated by the differences between the neutral and anionic (deprotonated) phenols. Deprotonation decreases the activation barrier for the 1,2-shift from 15 to 9 kcal mol^{-1}.

Natural bonding orbital (NBO) analysis[59] provides direct evidence for a very strong through-space interaction between the phenolate moiety and the back lobe of the σ* orbital of the breaking C–S bond in the 1,2-shift TS. Furthermore, the evolution of electron density in the participating functional groups clearly shows that the remote oxygen loses electron density in the 1,2-shift TS (Scheme S3). Remarkably, this oxygen loses *ca*. 6 times more density than the enolate carbon adjacent to the migrating group (Δq = 0.091e *vs*. 0.014e). These findings suggest that the nucleophilicity of the enolate plays only a secondary role in promoting the 1,2-shift (**Path I**), while the assistance from the phenoxide oxygen is of greater importance. These observations are also consistent with the transition state geometry: the C–Ar bond is just starting to break and the reaction at this stage can be better described as the beginning of cyclopropane formation *via* the phenoxide moiety (**Path III**).

However, as the intrinsic reaction coordinate (IRC) clearly shows that this process is aborted after the TS when the structure evolves further along the 1,2-shift path (**Path I**). Hence, the **Paths I** and **III** are intertwined – they cross in the multivariable reaction space by following a trajectory which benefits from the phenoxide electron density while preserving aromaticity.

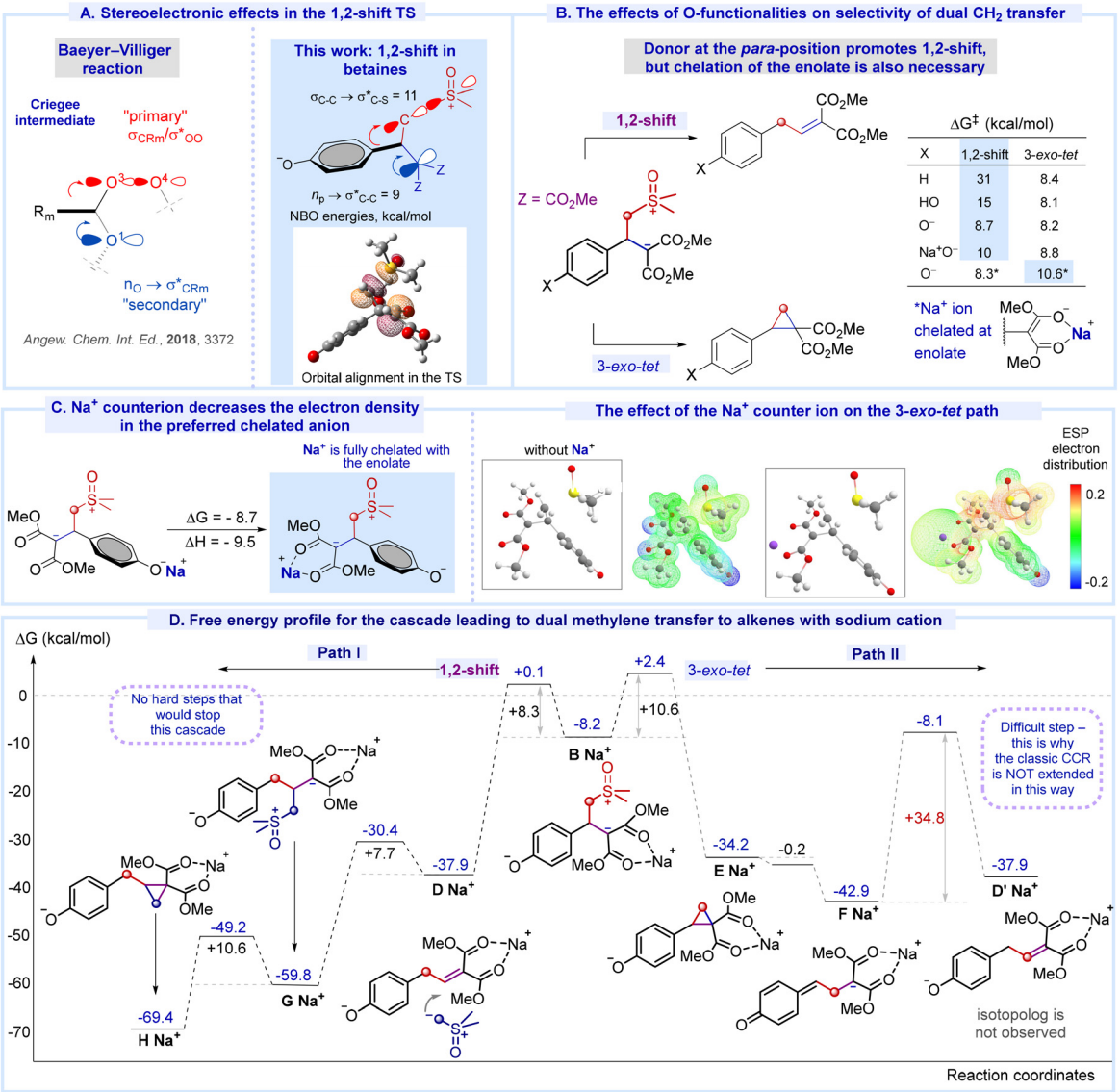

Fig. 1 A. Comparison of the two stereoelectronic effects in the Criegee intermediate of BVR and in the intermediate of 1,2-shift under discussion. B. Importance of the phenoxide moiety: dual methylenation is only possible with a strong donor group. Without such a donor, the first methylene insertion *via* the 1,2-shift is impossible. C. Sodium chelation by the enolate B is favored, which changes the electron density and decelerates the 3-*exo*-*tet* path (II). D. Free energy profile of the dual methylene transfer, including sodium cation, is in full agreement with experimental results.

Scheme 4 Proposed mechanism for 3-indolyl and 3-pyrrolyl-substituted alkenes.

This analysis has important practical implications. Since the enolate primarily drives the 3-*exo-tet* cyclization (**Path II**), it is reasonable to hypothesize that a partial deactivation of the enolate center could shift the competition between **Path I** and **Path II**. Enolate reactivity can vary significantly depending on structural factors.[60] Hence, as the next step, we analyzed how the sodium counterion can influence the enolate reactivity.

The role of the Na^+ counterion

Although each anionic center can coordinate with a Na^+ counterion, coordination at the diester enolate results in a chelated structure, which is energetically favored by 8.7 kcal mol^{-1} (Fig. 1C). Although one should treat this value as approximate since solvent molecules are not included in this model, this value suggests an equilibrium constant of approximately 10^6 for sodium cation transfer from the phenoxide to the enolate, indicating that sodium is fully chelated with the enolate.

In the presence of chelated Na^+ counterion, both electron density and nucleophilicity at the enolate are decreased. This effect is illustrated by the electrostatic potential maps. This change affects the 3-*exo-tet* cyclization (**Path II**) more than the 1,2-shift (**Path I**). Our calculations found that, while the barrier for **Path II** increases by 2.4 kcal mol^{-1}, the barrier for **Path I** remains largely unchanged. As a result of chelation, **Path I** is favored by 2.3 kcal mol^{-1}, and the final energy profile of the CH_2 insertion process is in full agreement with the experimental results (Fig. 1D).

The reduced yield of the target product in the presence of a potassium-containing base, along with its inefficiency when using a cesium-derived base (see SI), highlights the important role of the sodium ion. The larger potassium cation forms a weaker complex with the dialkyl malonate moiety, which increases the proportion of undesired pathways when potassium *tert*-butoxide is used. The even larger cesium cation is also unable to effectively interact with the malonate group, leading to a significant drop in the efficiency of the desired transformation. Consequently, the use of K- and Cs-derived bases results in lower product yields.

The proposed mechanism including the role of sodium cation explains well the results obtained during the variation of the substrate nature. Thus, moderate yields for halogen-containing substrates **1f–h** and low yield of 3,5-dibromo-4-hydroxybenzylcyclopropane **3i** can be explained by a negative inductive effect of halogen atoms that decreases an electron density on the phenoxy oxygen making 1,2-aryl shift less competitive with the malonate ion. Similarly, an acceptor group at the C(5) atom of the indole ring in **1u,v** decreases an electron density on the indole nitrogen and, as a result, the reactivity of the C(3) atom of the indole ring leading to the lower contribution of the 1,2-aryl shift. This effect is the most pronounced for 4-hydroxy-3-nitrophenyl-substituted substrates **1w,x,** the deprotonated form of which exists in quinonoid form with the negative charge localized at the nitro group. This explains the formation of arylcyclopropanes **5a,b** in the reactions of these substrates. On the other hand, the reason for the diminished yields of cyclopropanes **3l,m** is the weaker binding of sodium cation to phosphonoacetate and, especially, cyanoacetate in comparison to that with the malonate moiety. Therefore, the deceleration of the intermediate **B-Na**$^+$ transformation to the corresponding arylcyclopropane **E-Na**$^+$ is smaller than that for malonate, and 1,2-aryl shift is less competitive again.

Dual methylene transfer to aldehydes: homologation followed by epoxide formation

To expand the scope of the new dual methylene group transfer reaction, we explored another class of substrates commonly used in the CCR – aldehydes. We were glad to find that 4-hydroxybenzaldehydes **2** were successfully transformed into benzyloxiranes **4** (Scheme 5), which can serve as valuable precursors for various drugs, cosmetic agents, and bioactive molecules (Fig. 2).

For optimization of reaction conditions, we selected 4-hydroxybenzaldehyde **2a**. The results of this optimization are given in the Table S2. The best yield of **4a** was obtained with dimethylsulfonium methylide (DMSM) using a stepwise procedure including: (a) the preliminary deprotonation of the **2a** using NaH in DMSO at room temperature; (b) addition of trimethylsulfonium iodide (2.3 equiv.) to the reaction mixture at 40 °C; (c) subsequent *in situ* generation of the ylide by the dropwise addition of 1.5 M solution of *t*-BuOK (2.5 equiv.) in DMSO; and (d) stirring of the mixture at the same temperature for 30 min.

Under these conditions, we explored the scope of the new reaction and synthesized a series of (4-hydroxybenzyl)oxiranes **4**. Like the results for benzylcyclopropanes **3**, substrates with a halogen, alkyl or alkoxy groups at the C(3) and C(5) positions of 4-hydroxybenzaldehyde yielded the corresponding dual methylene transfer products in good to excellent yields

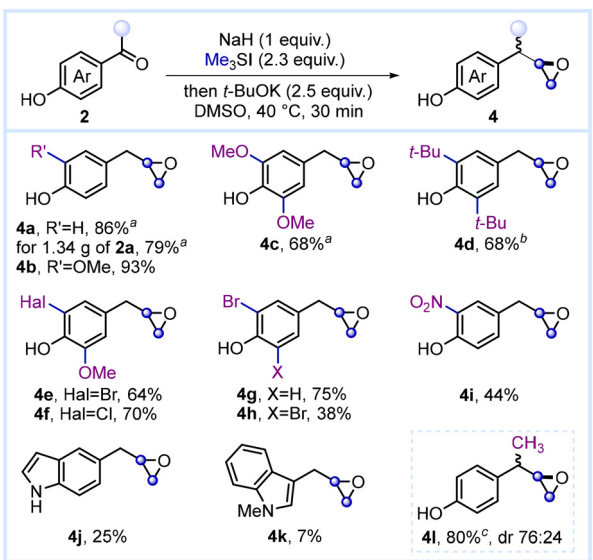

Scheme 5 Substrate scope for the dual methylene group transfer to aldehydes and ketones. [a] Reaction time – 1 h. [b] 3.5 equiv. of Me_3SI, 4.5 equiv. of *t*-BuOK, rt, 1 h. [c] Yield is based on the consumption of the starting material.

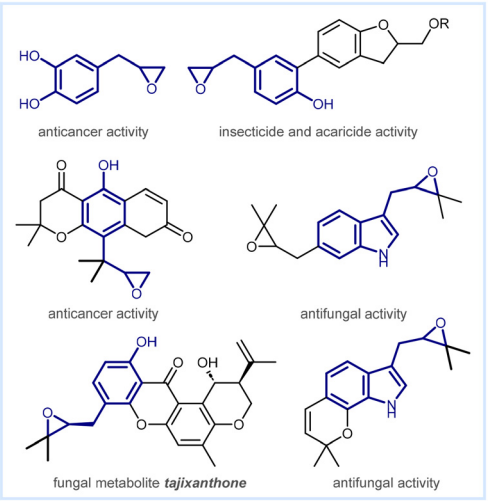

Fig. 2 Examples of bioactive 4-hydroxybenzyloxiranes.

(64–93% for **4b–g**); a gram-scale synthesis exemplified by **2a** transformation also provided the product in a good yield (Scheme 5). Interestingly, 3-nitro group did not suppress this reaction completely; product **4i** was obtained in 44% yield. Similarly, 5-formylindole produced the corresponding 2-(arylmethyl)oxirane **4j**, albeit in low yield (25% *vs.* no product from the corresponding benzylidenemalonate **1z**). Indole-3-carbaldehyde also participated in this reaction to give product **4k** resulting from both dual methylene transfer and *N*-methylation, albeit in only 7% yield. At last, not only aldehydes but also alkyl aryl ketones can be involved in the process of dual methylene group transfer. The reaction of DMSM with 4′-hydroxyacetophenone afforded the corresponding oxirane **4l** in good yield (80%) but as a mixture of two diastereomers in *ca.* 3 : 1 ratio.

While the dual methylene transfer to aldehydes also incorporates two CH_2 units, the reaction of perdeuterated DMSM with **2a** yielded the products with a different isotopic distribution. In contrast to the preparation of **3a-*d*$_4$**, the resulting oxirane ring in **4a-*d*$_3$** contains three deuterium atoms in the oxirane ring, with only one deuterium present at the benzylic carbon atom (Scheme 6A). The results of these experiments suggest that the reaction mechanisms for the formation of cyclopropanes **3** and oxiranes **4** are different. Indeed, after the slow, rate-determining ($\Delta G^{\ddagger}$ = +19.3 kcal mol^{-1}), and reversible nucleophilic attack of the ylide on the carbonyl moiety with the formation of a betaine intermediate **J**, the two competing irreversible pathways diverge (Scheme 6B).

Hence, despite the similar outcome, the new homologation reaction for alkenes and aldehydes takes a different direction at the fork between **Paths I** and **II**. Alkenes follow the 1,2-shift path while aldehydes prefer the 3-*exo-tet* direction. This is fortuitous for the dual methylene transfer to alkene because it avoids a deep kinetic trap that would wait on **Path II** (**F** → **D′** conversion, Fig. 1D) but inconsequential for the aldehyde reaction where an analogous step (**L** → **M** conversion, Scheme 6B) is fast and exergonic. However, in both cases, the presence of anionic oxygen substituent in the reactant is instrumental in unlocking this new reactivity. In a full agreement with the deuterium-labeling experiments, the barrier for the 1,2-shift (**Path I**) is higher than the barrier for the 3-*exo-tet* cyclization (**Path II**) by 4.1 kcal mol^{-1}, a key difference from the alkene reaction (Scheme 6B).

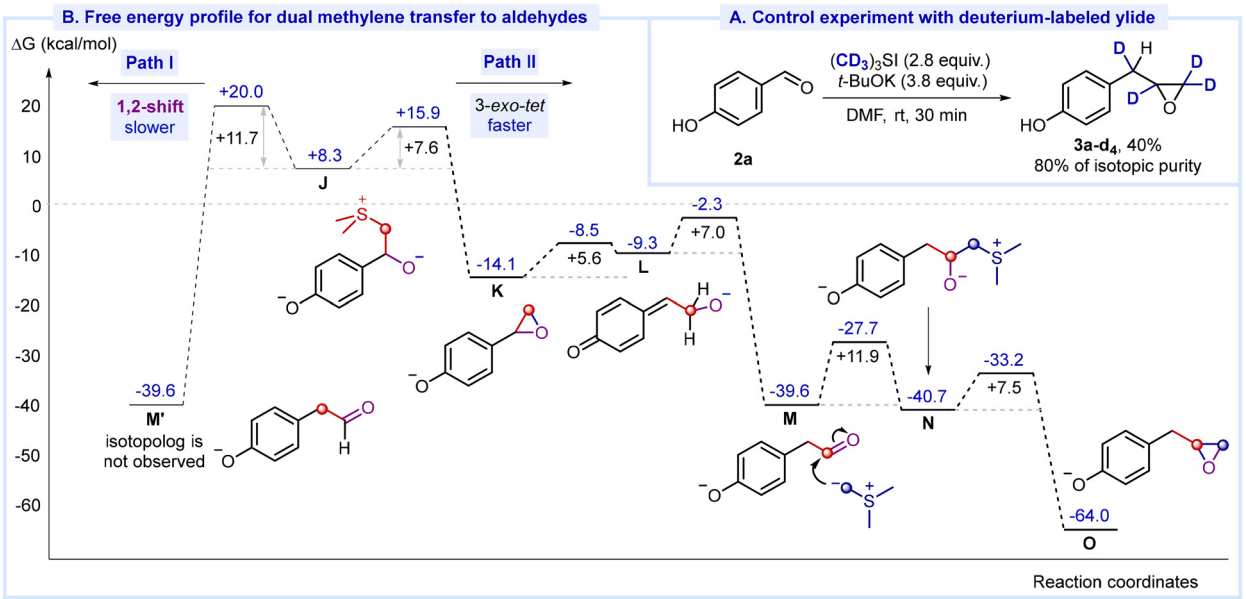

Scheme 6 A. Reaction of perdeuterated DMSM with 4-hydroxybenzaldehyde. B. Free energy profiles for the cascades leading to the extended CCR–isomerization–CCR sequence for 4-hydroxybenzaldehydes.

General implications for reaction design

The key feature of this reaction design is based on electron flow from a donor to an acceptor, mediated by a breaking C–C bond. This is, of course, a common motif in organic chemistry, but the present case has its own interesting features. To illustrate the reasons for the efficiency of this 1,2-shift, let's compare it with Grob fragmentations, another class of reactions driven by the same principle but featuring a different orbital topology.

In a typical Grob fragmentation, electron flow from the donor (D) to the acceptor (A) (Scheme 7, top-left) results in the formation of a C=D double bond at the expense of central C–C bond cleavage. The three participating orbitals—those of the donor, the breaking bond, and the acceptor—are arranged in a coplanar zigzag geometry to ensure effective overlap for the electron flow.[61–64]

However, this exact arrangement becomes impossible when one carbon is removed from the bridge, so the donor and acceptor are attached to the same carbon atom. In such cases, the electronic orbitals that constitute the C–R bond associated with the migrating group R act as a relay connecting the donor and the acceptor. During the migration, R "leaves behind" an empty partner orbital to form the C=D bond while simultaneously carrying along the electron density required to displace the leaving acceptor group X (Scheme 7, top-right).

In the 1,2-shift, the ultimate driving force remains the transfer of electron density from the donor to the acceptor, and the coplanarity of the orbitals remains essential for stereoelectronic reasons. However, the orbital arrangement differs here: instead of the antiperiplanar zigzag topology observed in Grob fragmentations, the donor/acceptor orbitals in the 1,2-shifts adopt a U-shaped geometry, accommodating the shorter bridge.

One could also mention that our 1,2-shift is stereoelectronically similar to the House-Meinwald rearrangement, except that the latter involves highly reactive carbocationic species.[63–71] In contrast, the 1,2-shift in our system is assisted by the enhanced electronic push from anionic species, which eliminates the need for a carbocation. The combination of a strong donor and a good leaving group, such as sulfide or sulfoxide, can efficiently drive the rearrangement when supported by two additional factors. First, reducing the electron density at the anionic center **D** (Scheme 7, bottom right) through cation chelation diminishes the likelihood of a "short-circuit" *via* direct donor–acceptor interaction that would lead to the 3-*exo-tet* cyclization and premature cyclopropanation. Second, the presence of a remote anionic group on the migrating substituent R enhances its migratory aptitude, as illustrated by the 16 kcal mol^{-1} drop in the activation barrier upon deprotonation (Fig. 1B).

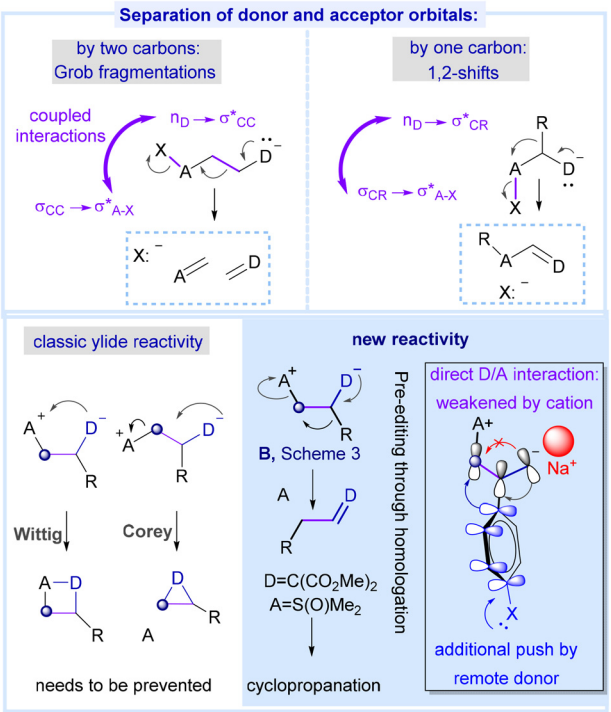

Scheme 7 Top: electron density finds a way to flow from a donor to an acceptor, even if it results in C–C bond scissions. Depending on the topology (vicinal *vs.* geminal), this leads either to Grob fragmentations or C–R scissions with migrations. Bottom: the new directions of betaine reactivity allow to reform the π-bond after homologation, paving the way for the classic Corey–Chaykovsky cyclopropanation and epoxidation to occur as the following step. The insert also shows the cooperative effect of two charge moderating interactions: chelation of the Na cation (red) at the enolate makes direct through-space donor–acceptor interaction leading to "unproductive" 3-*exo-tet* cyclization (and classic CC reaction) unfavorable while increased donation from the *para*-substituent X (blue) facilitates the 1,2-Ar shift.

Conclusions

The unexpected extension of the classic Corey–Chaykovsky reaction shows the possibility of homologative "*n* + 1 editing" *via* selective CH_2-insertion into a C–C bond before the reaction embarks on the classic cyclopropanation/epoxidation paths. In the newly discovered process, the ylide reagents play two distinctly different roles but, in both of these roles, they serve as a synthetic equivalent of a carbene.

Although the scope of this C–C insertion is relatively narrow now, the flip side of this scope is high selectivity. Such selectivity is particularly crucial for C–C insertions, given that typical organic molecules contain numerous C–C bonds. If many bonds were affected, the insertion would lack practical utility for precise molecular editing. However, the presence of a donor substituent in the Ar group allows methylene insertion to proceed with surgical precision. Both OH and NH functionalities can be deprotonated to switch on the nucleophilic anchimeric assistance to the 1,2-shift, thus avoiding the "normal" Corey–Chaykovsky cyclopropanation and enabling a new reactivity direction for the key betaine intermediate. Furthermore, this new ability of such ylides is made possible by the tightly coordinated network of stereoelectronic inter-

actions, which points out to the general design principles for carbenoid insertions and other synthetic applications of the anionic 1,2-shifts.

We hope that the previously unknown pattern of ylide reactivity will stimulate the search for other substrates for the implementation of dual methylene transfers and lead to the discovery of related processes containing similar insertion of diverse carbenoids and their heteroatom analogues into the C–C bonds. Further extensions of this new "two-in-one" methodology for construction of small rings coupled with chain elongation are under investigation.

Author contributions

All authors took part in the conceptualisation of this study. S. V. V., N. A. A. carried out the experimental work. Z. S. S. carried out NMR studies. S. V. V., A. I. A. and R. N. K. wrote the SI. C. B. K. and A. I. V. performed the DFT calculations. S. V. V., A. I. A., T. I. V., I. O. A. and A. I. V. wrote the original draft of the manuscript. All authors contributed to the final version of the manuscript.

Conflicts of interest

There are no conflicts to declare.

Data availability

Experimental and computational details are available on demand from authors.

Supplementary information (SI) is available. See DOI: **https://doi.org/10.1039/d5qo01266j**.

CCDC 2179907 contains the supplementary crystallographic data for this paper.[72]

Acknowledgements

The study was supported by Russian Science Foundation, project 25-73-20019 (I. O. A.). The computational work at FSU was supported by the National Science Foundation (NSF) (CHE-2102579) and used the Indiana Jetstream2 at Indiana University through allocation CHE240023 from the ACCESS Program, further supported by NSF grants #2138259, #2138286, #2138307, #2137603 and #2138296. C. B. K. is grateful for the support received from the ACM SIGHPC Computational and Data Fellowship.

References

1 V. H. Gessner, *Modern Ylide Chemistry. Applications in Ligand Design, Organic and Catalytic Transformations*, Springer Cham, Switzerland, 2018.

2 S. Kumar, V. Borkar, M. Mujahid, S. Nunewar and V. Kanchupalli, Iodonium ylides: an emerging and alternative carbene precursor for C–H functionalizations, *Org. Biomol. Chem.*, 2023, **21**, 24–38.

3 P. Bhorali, S. Sultana and S. Gogoi, Recent Advances in Metal-Catalyzed C–H Bond Functionalization Reactions of Sulfoxonium Ylides, *Asian J. Org. Chem.*, 2022, **11**, e202100754.

4 A. Kumar, M. S. Sherikar, V. Hanchate and K. R. Prabhu, Application of sulfoxonium ylide in transition-metal-catalyzed C–H bond activation and functionalization reactions, *Tetrahedron*, 2021, **101**, 132478.

5 S. Jana, Y. Guo and R. M. Koenigs, Recent Perspectives on Rearrangement Reactions of Ylides via Carbene Transfer Reactions, *Chem. – Eur. J.*, 2021, **27**, 1270–1281.

6 E. J. Corey and M. Chaykovsky, Dimethyloxosulfonium Methylide ($(CH_3)_2SOCH_2$) and Dimethylsulfonium Methylide ($(CH_3)_2SCH_2$). Formation and Application to Organic Synthesis, *J. Am. Chem. Soc.*, 1965, **87**, 1353–1364.

7 E. J. Corey and M. Chaykovsky, Dimethylsulfonium Methylide, A Reagent for Selective Oxirane Synthesis from Aldehydes and Ketones, *J. Am. Chem. Soc.*, 1962, **84**, 3782–3783.

8 E. J. Corey and M. Chaykovsky, Dimethylsulfoxonium Methylide, *J. Am. Chem. Soc.*, 1962, **84**, 867–868.

9 G. L. Beutner and D. T. George, Opportunities for the Application and Advancement of the Corey–Chaykovsky Cyclopropanation, *Org. Process Res. Dev.*, 2023, **27**, 10–41.

10 Homologation of aldehydes including oxirane formation under treatment with sulfur ylides followed by (Lewis) acid-induced oxirane rearrangement into new aldehyde is known, for example: A. Delbrassinne, B. J. Takam Mba, L. Collard and R. Robiette, One-Carbon Homologation of α,β-Unsaturated Aldehydes: Access to α-Tertiary β,γ-Unsaturated Aldehydes, *Eur. J. Org. Chem.*, 2023, **26**, e202300765. However, this and other stepwise transformations cannot be considered as direct ylide insertion into C–C bond.

11 M.-Y. Huang and S.-F. Zhu, Uncommon carbene insertion reactions, *Chem. Sci.*, 2021, **12**, 15790–15801.

12 S. Li, C. Zhang, G. Pan, L. Yang, Z. Su, X. Feng and X. Liu, Enantioselective Photochemical Carbene Insertion into C–C and C–H Bonds of 1,3-Diketones by a Guanidine-Amide Organocatalyst, *ACS Catal.*, 2023, **13**, 4656–4666.

13 Y. Wu, Y. Ning, X. Han, P. Liao, Y. Xia, P. Sivaguru and X. Bi, Silver-Catalyzed Vinylcarbene Insertion into C–C Bonds of 1,3-Diketones with Vinyl-*N*-triftosylhydrazones, *Org. Lett.*, 2022, **24**, 8136–8141.

14 Z. Liu, X. Zhang, M. Virelli, G. Zanoni, E. A. Anderson and X. Bi, Silver-Catalyzed Regio- and Stereoselective Formal Carbene Insertion into Unstrained C–C σ-Bonds of 1,3-Dicarbonyls, *iScience*, 2018, **8**, 54–60.

15 V. K. Aggarwal, J. N. Harvey and R. Robiette, On the Importance of Leaving Group Ability in Reactions of Ammonium, Oxonium, Phosphonium and Sulfonium Ylides, *Angew. Chem., Int. Ed.*, 2005, **44**, 5468–5471.

16 J. B. Bapat, J. Epsztajn, A. R. Katritzky and B. Plau, *N*-oxides and related compounds. Part 58. Some precursors of pyridinium methylide, *J. Chem. Soc., Perkin Trans. 1*, 1977, 1692–1697.
17 F. Kröhnke, Synthese von Pyridinium-äthanolen durch eine neuartige Aldehyd-Kondensation, *Chem. Ber.*, 1934, **67B**, 656–667.
18 L. D. Funt, M. S. Novikov and A. F. Khlebnikov, New applications of pyridinium ylides toward heterocyclic synthesis, *Tetrahedron*, 2020, **76**, 131415.
19 S. K. Shrivastava, P. Srivastava, R. Bandresh, P. N. Tripathi and A. Tripathi, Design, synthesis and biological evaluation of some novel indolizine derivatives as dual cyclooxygenase and lipoxygenase inhibitor for anti-inflammatory activity, *Bioorg. Med. Chem.*, 2017, **25**, 4424–4432.
20 D. S. Allgäuer and H. Mayr, One-Pot Two-Step Synthesis of 1-(Ethoxycarbonyl)indolizines via Pyridinium Ylides, *Eur. J. Org. Chem.*, 2013, 6379–6388.
21 A. Sarbajna, V. S. V. S. N. Swamy and V. H. Gessner, Phosphorus-ylides: powerful substituents for the stabilization of reactive main group compounds, *Chem. Sci.*, 2021, **12**, 2016–2024.
22 O. I. Kolodiazhnyi, *Phosphorus ylides: chemistry and applications in organic synthesis*, Wiley-VCH, Weinheim, Germany, 1999.
23 C. A. D. Caiuby, L. G. Furniel and A. C. B. Burtoloso, Asymmetric transformations from sulfoxonium ylides, *Chem. Sci.*, 2022, **13**, 1192–1209.
24 G. D. Bisag, S. Ruggieri, M. Fochi and L. Bernardi, Sulfoxonium ylides: simple compounds with chameleonic reactivity, *Org. Biomol. Chem.*, 2020, **18**, 8793–8809.
25 L.-Q. Lu, T.-R. Li, Q. Wang and W.-J. Xiao, Beyond sulfide-centric catalysis: recent advances in the catalytic cyclization reactions of sulfur ylides, *Chem. Soc. Rev.*, 2017, **46**, 4135–4149.
26 R. O. Shcherbakov, D. A. Myasnikov, I. V. Trushkov and M. G. Uchuskin, Extended Version of the Corey–Chaykovsky Reaction: Synthesis of 2,4-Substituted Furans by the Treatment of β-Dialkylamino Chalcones with Dimethylsulfonium Methylide, *J. Org. Chem.*, 2023, **88**, 8227–8235.
27 A. A. Fadeev, A. S. Makarov, O. A. Ivanova, M. G. Uchuskin and I. V. Trushkov, Extended Corey-Chaykovsky reactions: transformation of 2-hydroxychalcones to benzannulated 2,8-dioxabicyclo[3.2.1]octanes and 2,3-dihydrobenzofurans, *Org. Chem. Front.*, 2022, **9**, 737–744.
28 A. O. Chagarovsky, E. M. Budynina, O. A. Ivanova, E. V. Villemson, V. B. Rybakov, I. V. Trushkov and M. Y. Melnikov, Reaction of Corey Ylide with α,β-Unsaturated Ketones: Tuning of Chemoselectivity toward Dihydrofuran Synthesis, *Org. Lett.*, 2014, **16**, 2830–2833.
29 B. Singh, A. J. Ansari, N. Malik and S. S. V. Ramasastry, An interrupted Corey-Chaykovsky reaction of designed azaarenium salts: synthesis of complex polycyclic spiro- and fused cyclopropanoids, *Chem. Sci.*, 2023, **14**, 6963–6969.
30 J. Chu, H. Wang and S. R. Wang, Steric Hindrance Tuned [4 + 1] Annulation of α-Substituted Conjugated Enones with Ylides for Dihydrofuran Synthesis, *Org. Lett.*, 2025, **27**, 86–90.
31 P. Banerjee and A. T. Biju, *Donor-Acceptor Cyclopropanes in Organic Synthesis*, Wiley-VCH, Weinheim, Germany, 2024.
32 L. Yang, H. Wang, M. Lang and S. Peng, Recent Advances on High-Order Dipolar Annulations of Donor–Acceptor Cyclopropanes/Cyclobutanes, *Synthesis*, 2024, 389–398.
33 F. Doraghi, S. Karimian, O. H. Qareaghaj, M. J. Karimi, B. Larijani and M. Mahdavi, Recent advances in ring-opening reactions of 2-substituted donor-acceptor cyclopropanes under metal catalysis, *J. Organomet. Chem.*, 2024, **1005**, 122963.
34 M. Bao and M. P. Doyle, Asymmetric [3 + n]-Cycloaddition Reactions of Donor-Acceptor Cyclopropanes, *ChemCatChem*, 2023, **15**, e202301090.
35 A. Deepthi, C. B. Meenakshy and M. Mohan, Synthesis of heterocycles from donor-acceptor cyclopropanes: a five-year recap, *Synthesis*, 2023, 3875–3894.
36 Y. Xia, X. Liu and X. Feng, Asymmetric Catalytic Reactions of Donor–Acceptor Cyclopropanes, *Angew. Chem., Int. Ed.*, 2021, **60**, 9192–9204.
37 K. Ghosh and S. Das, Recent advances in ring-opening of donor acceptor cyclopropanes using C-nucleophiles, *Org. Biomol. Chem.*, 2021, **19**, 965–982.
38 V. Pirenne, B. Muriel and J. Waser, Catalytic Enantioselective Ring-Opening Reactions of Cyclopropanes, *Chem. Rev.*, 2021, **121**, 227–263.
39 P. Singh, R. K. Varshnaya, R. Dey and P. Banerjee, Donor–acceptor cyclopropanes as an expedient building block towards the construction of nitrogen-containing molecules: an update, *Adv. Synth. Catal.*, 2020, **362**, 1447–1484.
40 T. F. Schneider, J. Kaschel and D. B. Werz, A New Golden Age for Donor–Acceptor Cyclopropanes, *Angew. Chem., Int. Ed.*, 2014, **53**, 5504–5523.
41 V. V. Shorokhov, B. K. Chabuka, T. P. Tikhonov, A. V. Filippova, S. S. Zhokhov, V. A. Tafeenko, I. A. Andreev, N. K. Ratmanova, M. G. Uchuskin, I. V. Trushkov, I. V. Alabugin and O. A. Ivanova, Converting Strain Release into Aromaticity Loss for Activation of Donor–Acceptor Cyclopropanes: Generation of Quinone Methide Traps for C-Nucleophiles, *Org. Lett.*, 2024, **26**, 8177–8182.
42 S. M. Antropov, S. A. Tokmacheva, I. I. Levina, O. A. Ivanova and I. V. Trushkov, Synthesis of Bridged Bicyclic Systems peri-Annulated to the Indole Ring: Tropane-Fused Indoles, *Adv. Synth. Catal.*, 2024, **366**, 2784–2790.
43 V. V. Shorokhov, S. S. Zhokhov, V. B. Rybakov, M. A. Boichenko, I. A. Andreev, N. K. Ratmanova, I. V. Trushkov and O. A. Ivanova, Donor–Acceptor Cyclopropane Ring Expansion to 1,2-Dihydronaphthalenes. Access to Bridged Seven-Membered Lactones, *Org. Lett.*, 2023, **25**, 7963–7967.
44 V. T. Abaev, I. V. Trushkov and M. G. Uchuskin, The Butin reaction, *Chem. Heterocycl. Compd.*, 2016, **52**, 973–995.

45 M. A. Boichenko, A. Y. Plodukhin, V. V. Shorokhov, D. S. Lebedev, A. V. Filippova, S. S. Zhokhov, E. A. Tarasenko, V. B. Rybakov, I. V. Trushkov and O. A. Ivanova, Synthesis of 1,5-Substituted Pyrrolidin-2-ones from Donor–Acceptor Cyclopropanes and Anilines/Benzylamines, *Molecules*, 2022, **27**, 8468.

46 M. N. Anisimov, M. A. Boichenko, V. V. Shorokhov, J. N. Borzunova, M. Janibekova, V. V. Mustyatsa, I. A. Lifshits, A. Y. Plodukhin, I. A. Andreev, N. K. Ratmanova, S. S. Zhokhov, E. A. Tarasenko, D. A. Ipatova, A. R. Pisarev, I. A. Vorobjev, I. V. Trushkov, O. A. Ivanova and N. B. Gudimchuk, Synthesis and evaluation of tetrahydropyrrolo[1,2-*a*]quinolin-1(2*H*)-ones as new tubulin polymerization inhibitors, *RSC Med. Chem.*, 2025, **16**, 274–285.

47 P. J. Stephens, F. J. Devlin, C. F. Chabalowski and M. J. Frisch, Ab Initio calculation of vibrational absorption and circular dichroism spectra using density functional force fields, *J. Phys. Chem.*, 1994, **98**, 11623–11627.

48 A. D. McLean and G. S. Chandler, Contracted Gaussian basis sets for molecular calculations. I. Second row atoms, Z = 11–18, *J. Chem. Phys.*, 1980, **72**, 5639–5648.

49 R. Krishnan, J. S. Binkley, R. Seeger and J. A. Pople, Self-consistent molecular orbital methods. XX. A basis set for correlated wave functions, *J. Chem. Phys.*, 1980, **72**, 650–654.

50 E. Caldeweyher, C. Bannwarth and S. Grimme, Extension of the D3 dispersion coefficient model, *J. Chem. Phys.*, 2017, **147**, 034112.

51 E. Caldeweyher, S. Ehlert, A. Hansen, H. Neugebauer, S. Spicher, C. Bannwarth and S. Grimme, A generally applicable atomic-charge dependent London dispersion correction, *J. Chem. Phys.*, 2019, **150**, 154122.

52 S. Miertuš, E. Scrocco and J. Tomasi, Electrostatic interaction of a solute with a continuum. A direct utilizaion of AB initio molecular potentials for the prevision of solvent effects, *J. Chem. Phys.*, 1981, **55**, 117–129.

53 S. Chandrasekhar and C. D. Roy, Conformationally Restricted Criegee Intermediates: Evidence for Formation and Stereoelectronically Controlled Fragmentation, *J. Chem. Soc., Perkin Trans. 2*, 1994, 2141–2143.

54 C. M. Crudden, A. C. Chen and L. A. Calhoun, A Demonstration of the Primary Stereoelectronic Effect in the Baeyer–Villiger Oxidation of α-Fluorocyclohexanones, *Angew. Chem., Int. Ed.*, 2000, **39**, 2851–2855.

55 V. A. Vil', G. dos Passos Gomes, O. V. Bityukov, K. A. Lyssenko, G. I. Nikishin, I. V. Alabugin and A. O. Terent'ev, Interrupted Baeyer–Villiger Rearrangement: Building A Stereoelectronic Trap for the Criegee Intermediate, *Angew. Chem., Int. Ed.*, 2018, **57**, 3372–3376.

56 V. A. Vil, Y. A. Barsegyan, L. Kuhn, M. V. Ekimova, E. A. Semenov, A. A. Korlyukov, A. O. Terent'ev and I. V. Alabugin, Synthesis of Unstrained Criegee Intermediates: Inverse α-Effect and Other Protective Stereoelectronic Forces Can Stop Baeyer–Villiger Rearrangement of γ-Hydroperoxy-γ-Peroxylactones, *Chem. Sci.*, 2020, **11**, 5313–5322.

57 I. V. Alabugin, *Stereoelectronic Effects: A Bridge Between Structure and Reactivity*, John Wiley & Sons, Chichester (UK), Hoboken (USA), 2016.

58 I. Alabugin and L. Kuhn, *Oxygen: The Key to Stereoelectronic Control in Chemistry*, ACS In Focus, American Chemical Society, 2023.

59 E. D. Glendening and F. Weinhold, Natural Resonance Theory: II. Natural Bond Order and Valency, *J. Comput. Chem.*, 1998, **19**, 610–627.

60 A. I. Leonov, D. S. Timofeeva, A. R. Ofial and H. Mayr, Metal Enolates – Enamines – Enol Ethers: How Do Enolate Equivalents Differ in Nucleophilic Reactivity?, *Synthesis*, 2019, 1157–1170.

61 C. A. Grob and W. Baumann, Die 1,4-Eliminierung unter Fragmentierung, *Helv. Chim. Acta*, 1955, **38**, 594–610.

62 C. J. Laconsay, K. Y. Tsuia and D. J. Tantillo, Tipping the balance: theoretical interrogation of divergent extended heterolytic fragmentations, *Chem. Sci.*, 2020, **11**, 2231–2242.

63 J. Y. Yang, T. T. Hoang and G. B. Dudley, Alkynogenic fragmentation, *Org. Chem. Front.*, 2019, **6**, 2560–2569.

64 I. V. Alabugin, L. Kuhn, M. G. Medvedev, N. V. Krivoshchapov, V. A. Vil', I. A. Yaremenko, P. Mehaffy, M. Yarie, A. O. Terent'ev and M. A. Zolfigol, Stereoelectronic Power of Oxygen in Control of Chemical Reactivity: the Anomeric Effect is not Alone, *Chem. Soc. Rev.*, 2021, **50**, 10253–10345.

65 H. O. House, The acid-catalyzed rearrangement of the stilbene oxide, *J. Am. Chem. Soc.*, 1955, **77**, 3070–3075.

66 J. Meinwald, S. S. Labana and M. S. Chadha, Peracid reactions. III. The oxidation of bicyclo[2.2.1]heptadiene, *J. Am. Chem. Soc.*, 1963, **85**, 582–585.

67 Y. Zhang, B. Hu, Y. Chen and Z. Wang, Review on Catalytic Meinwald Rearrangement of Epoxides, *Chem. – Eur. J.*, 2024, **30**, e202402469.

68 C. F. Lee, D. B. Diaz, A. Holownia, S. J. Kaldas, S. K. Liew, G. E. Garrett, T. Dudding and A. K. Yudin, Amine hemilability enables boron to mechanistically resemble either hydride or proton, *Nat. Chem.*, 2018, **10**, 1062–1070.

69 J. A. Law, D. P. Callen, E. L. Paola, G. Gomes and J. H. Frederich, A Stereoselective Photoinduced Cycloisomerization Inspired by Ophiobolin A, *Org. Lett.*, 2022, **24**, 6499–6504.

70 F. Dressler, V. Öhler, C. Topp and P. R. Schreiner, Organocatalytic, Chemoselective, and Stereospecific House–Meinwald Rearrangement of Trisubstituted Epoxides, *Synlett*, 2024, 1052–1056.

71 N. Jeedimalla, C. Jacquet, D. Bahneva, J.-J. Y. Tendoung and S. P. Roche, Synthesis of α-Arylated Cycloalkanones from Congested Trisubstituted Spiro-epoxides: Application of the House–Meinwald Rearrangement for Ring Expansion, *J. Org. Chem.*, 2018, **83**, 12357–12373.

72 CCDC 2179907: Experimental Crystal Structure Determination, 2025, DOI: **10.5517/ccdc.csd.cc2c5clj**.